A Spatially-Constrained Color–Texture Model for Hierarchical VHR Image Segmentation

Zhongwen Hu, Zhaocong Wu, Qian Zhang, Qian Fan, and Jiahui Xu

***Abstract*—This letter presents a novel spatially-constrained color–texture model for hierarchical segmentation of very high resolution images. The segmentation starts with an initial partition, where the image is partitioned into many homogeneous regions. Then, the regions are regarded as node sets of a region adjacency graph, in which the distances of each pair of adjacent regions are calculated combining color and textural features with spatial constraint. Finally, a stepwise optimized region merging process is applied to obtain hierarchical segmentation results. Experiments and comparisons by using different satellite images are carried out to demonstrate the encouraging performance as well as the high efficiency of the proposed method.**

***Index Terms*—Color–texture segmentation, hierarchical region merging, hierarchical stepwise optimization (HSWO), local binary patterns (LBPs), remote sensing images, spatial constraint.**

I. Introduction

IMAGE segmentation is a key step in object-oriented remote sensing applications [1], such as object-based classification and change detection. It is used with the expectation that it will divide the image into semantically significant regions, or objects, to be recognized by further processing steps [2]. This work has attracted thousands of researchers in the past decade but is still an intractable problem [3]. According to the features utilized in different methods, segmentation methods can be cataloged into three types: spectral-based methods, texture-based methods, and spectral–texture combined methods [3]. Although some spectral- or texture-based segmentation methods have been proved effective in segmenting remote sensing images [4]–[6], it is proved that color–texture combined methods produce more reliable and accurate segmentation results among [3], [7], and [8]. Many spectral–texture segmentation methods proposed in the past few years had produced encouraging results; however, there still exist some limitations applied to remote sensing images.

Manuscript received September 10, 2011; revised December 10, 2011 and February 21, 2012; accepted April 2, 2012. This work was supported in part by the National High Technology Research and Development Program of China under Grant 2007AA12Z143, by the National Natural Science Foundation under Grants 40201039 and 40771157, and by the Fundamental Research Funds for the Central Universities under Grants 20102130201000134, 201121302020003, and 2011QD03.

Z. Hu, Z. Wu, Q. Zhang, and Q. Fan are with the School of Remote Sensing and Information Engineering, Wuhan University, Wuhan 430079, China (e-mail: zhongwenhu@163.com; zcwoo@whu.edu.cn; hangfanzq@163.com; fanqian86@gmail.com).

J. Xu is with the School of Geographic and Oceanographic Sciences, Nanjing University, Nanjing 210093, China (e-mail: amy_8688@126.com).

Color versions of one or more of the figures in this paper are available online at http://ieeexplore.ieee.org.

Digital Object Identifier 10.1109/LGRS.2012.2194693

Some complex models have been developed for segmenting nature and synthetic images, such as the J-images segmentation (JSEG) [9], Gaussian mixture models [10], and Markov random fields [11]. However, these methods will meet innate theoretical limitations or poor efficiency when applied to remote sensing images, which are very complex and containing thousands of different objects. Moreover, some other methods combining different textural features with color features were proposed, such as the Gabor [3] and wavelet [12] textural features. These methods were proved effective in segmenting remote sensing images but suffered poor efficiency in extraction of textures.

In recent years, a theoretically simple but effective texture descriptor named local binary patterns (LBPs) has been developed for texture description [13], [14]. It was introduced to color–texture segmentation of nature and synthetical images by Chen and Chen [15] and further developed for color–texture segmentation of remote sensing images [7], [8]. However, this kind of methods is limited by the blocklike initial partition, which leads to the inability to combine spatial features (such as geometric features). In addition, the size of each block is limited to be no less than 16×16 pixels in order to keep the stability of color and textural features, but this is not applicable for segmenting narrow ribbonlike objects, whose width would be much smaller than the block size.

In this letter, a novel spatially-constrained color–texture model is introduced to hierarchical segmentation of very high resolution (VHR) images. For a given image, the method starts with an initial partition, followed by a representation of the regions using a region adjacency graph (RAG) [16], in which a novel spatially-constrained color–texture model is used to measure the distances between adjacent regions. Finally, the RAG-based hierarchical stepwise optimized region merging process [17] is then applied to obtain hierarchical representations, which are not only useful for efficient algorithmic implementation but also can give important information on the relations between the regions in the image.

This letter is organized as follows: In Section II, the hierarchical image segmentation framework used in the proposed method is described; the spatially-constrained color–texture model is described in Section III, which is divided into three progressive sections; experimental results and discussions are presented in Section IV; the conclusion is drawn in Section V.

II. Hierarchical Image Segmentation

In this section, we describe the hierarchical segmentation model utilized in the proposed method. In this approach, the hierarchical stepwise optimization (HSWO) approach proposed by Beaulieu and Goldberg [17] is adopted, which employs a sequence of optimization processes to produce hierarchical

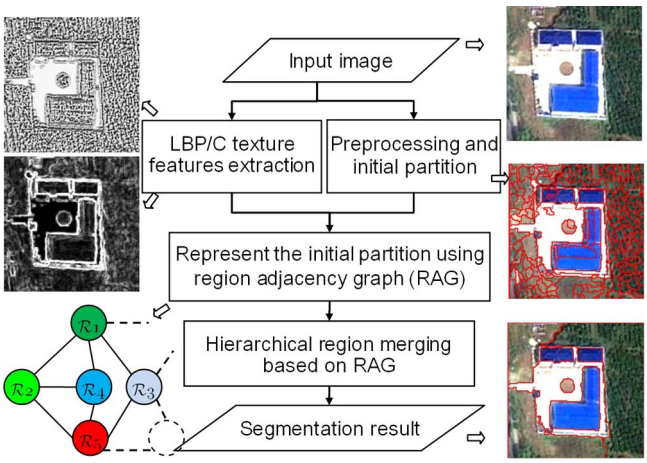

Fig. 1. Workflow of the proposed method.

segmentation results of different levels of details, and has been widely used for analysis of remote sensing images [5], [18]. The proposed approach starts with an initial partition; meanwhile, the local binary patterns/contrast (LBP/C) texture images are computed. Moreover, then, the regions are represented as node sets of the RAG [17]. An edge exists between two nodes when the two regions are adjacent, where the weight of the edge corresponds to the distance of the two regions. Finally, a RAG-based hierarchical stepwise optimized merging procedure is carried out to get the hierarchical segmentation results.

There are three main steps in the approach, and the flowchart of the proposed approach is shown in Fig. 1.

1) Initial partition and textural feature extraction. In this step, the edge embedded marker-based watershed (EEMW) [19] algorithm is utilized to produce the initial partition, and meanwhile, LBP/C textural features are extracted.
2) Representation of the initial partition using RAG [16]. Regions of the initial partition are represented as node sets of an undirected graph. The weights of the edges represent the costs of merging the corresponding pair of regions.
3) Hierarchical region merging based on RAG. In this step, the iterative merging process is applied, and at each iteration, two segments with minimal merging cost are merged to yield a segment hierarchy. Finally, hierarchical segmentation results can be obtained when the merging process is terminated by the given threshold.

In the hierarchical merging procedure, the HSWO process is used to select the segment pair that minimizes a stepwise criterion $C_{m,n}$, corresponding to the cost of merging m with n, which is similar to the merging importance in [8] and [13]. Following Beaulieu's optimization process [17], the merging cost utilized in this letter is defined as

$$C_{m,n} = \frac{S_m S_n}{S_m + S_n} D_{m,n} \tag{1}$$

where S_m and S_n denote the areas of m and n and $D_{m,n}$ denotes their distance in feature space. The distance $D_{m,n}$, which represents the distance of two segments, is calculated using the proposed distance model described in Section III.

III. Spatially-Constrained Color–Texture Model

In this section, we introduce the spatially-constrained color–texture distance model used in the region merging process.

A. Rotation-Invariant LBPs

The textural features used in the proposed approach are characterized by the joint distribution of LBP and local contrast features. It is computationally simple and robust in detecting texture structures. The LBP operator describes the structure of 3×3 neighborhoods, while the local contrast describes the textural intensity. The neighbor pixels are thresholded by the value of the center pixel and then multiplied by the binomial weights given to the corresponding pixels. The obtained values are summed as the LBP value of this texture unit. It is defined as follows:

$$LBP_{P,R} = \sum_{p=0}^{P-1} 2^p s_p, \qquad \text{where} \quad s_p = \begin{cases} 0, & g_p < g_c \\ 1, & g_p \geq g_c \end{cases} \tag{2}$$

where P is the number of neighboring pixels on a circle of radius R; g_p and g_c denote the image intensity values of the pth neighbor and the center pixel, respectively; and s_p is a binary flag denoting the relation of g_p and g_c. The calculation of LBP is clearly described in [13].

Since the weights for each neighbor are fixed, the original LBP is sensitive to texture rotation. In order to achieve rotation-invariant texture descriptor, Ojala *et al.* [14] proposed the rotation-invariant LBP, where a series of LBP values can be obtained by rotating the neighbor pixels and the minimum is selected as the final LBP value. This can be defined as

$$LBP^{ri}_{P,R} = \min\{ROR(LBP_{P,R}, i) | i = 0, 1, \ldots, P-1\} \tag{3}$$

where $ROR(x, i)$ performs a circular bitwise right shift on the P-bit number x for i times. For a 3×3 local window, there are eight neighborhoods and only 36 possible values for rotation-invariant LBP.

LBP is a gray-scale-invariant measure which addresses the spatial structure of the local texture. Since the LBP is proposed as a complementary measure, local contrast should be incorporated to measure the texture. The gray-scale-invariant measure proposed in [14] is used as a local contrast in this letter

$$LC_{P,R} = \frac{1}{P} \sum_{p=0}^{P-1} (g_p - \mu)^2, \qquad \text{where} \quad \mu = \frac{1}{P} \sum_{p=0}^{P-1} g_p. \tag{4}$$

The joint distribution of $LBP_{P,R}/LC_{P,R}$ is expected to be a very powerful rotation-invariant measure of local image texture.

B. Weighted Color–Texture Model

In this method, the color distance of two regions is computed using their color histograms, and the texture distance is computed using the joint histograms of LBP and local contrast. To avoid making any possible erroneous assumptions about the feature distributions, the nonparametric statistical method should be used to measure the distance of two distributions. In our study, the G-statistic [14], which is a modification of

Kullback–Leibler distance, is used to measure the distance of two histograms m and n. It is defined as follows:

$$G_{m,n} = \left\{ \sum_{m,n} \sum_{i=0}^{t-1} f_i \log f_i + \left(\sum_{m,n} \sum_{i=0}^{t-1} f_i \right) \log \left(\sum_{m,n} \sum_{i=0}^{t-1} f_i \right) - \sum_{m,n} \left(\sum_{i=0}^{t-1} f_i \right) \log \left(\sum_{i=0}^{t-1} f_i \right) - \sum_{i=0}^{t-1} \left(\sum_{m,n} f_i \right) \log \left(\sum_{m,n} f_i \right) \right\} \quad (5)$$

where t denotes the number of bins in the histograms and $G_{m,n}$ denotes the corresponding G-statistic value. Then, the color and texture distances can be obtained using their color and joint LBP/C histograms, respectively.

Moreover, then, the automatical combination of color and textural features is the key step for color–texture segmentation. In the proposed method, the color and textural distances are combined in a weighted way; it is defined as follows:

$$D_{m,n} = w_C G_C + w_T G_T \quad (6)$$

where $D_{m,n}$ denotes the combined distance of m and n; G_C and G_T denote the color and texture distances, respectively; and w_C and w_T are their corresponding weights. Then, the key point is how the weights w_C and w_T are determined.

In this letter, a totally automatical method for determining the weights is presented, similar to the method by Ilea and Whelan [20]. It is generally based on the assumption that, if the color distribution is homogeneous, the weights are adjusted in order to give the color information more importance. Conversely, if the color distribution is heterogeneous, it is assumed that the texture is the dominant feature, and the algorithm allocates more weight to texture. It is able to locally adapt to the image content by evaluating the uniformity of color distribution.

For an N-channel image, the weights for calculating the distance between m and n are defined as follows:

$$w_C = \sqrt{\min(k_m, k_n)}, \qquad \text{where} \quad k = \frac{1}{N} \sum_{i=0}^{N} \max(f_i) \quad (7)$$

$$w_T = 1 - w_C \quad (8)$$

where $\max(f_i)$ denotes the maximum of color frequency in the ith raster band and k_m and k_n are calculated from m and n, respectively.

C. Spatially-Constrained Color–Texture Model

Image segmentation is the process of partitioning an image into several constituent components that have similar characteristics [8]. However, most objects have their specific spatial patterns, particularly for textural areas. Segmentation using only color and textural features usually leads to meaningless objects with zigzag contours. A simple illusion can be seen in the first row of Fig. 2. Thus, it is necessary to exploit spatial constraint to obtain compact and meaningful objects. To incorporate with spatial features to improve the segmentation quality, it is assumed that the adjacent regions with longer shared boundary may belong to the same hierarchical parent with higher priority.

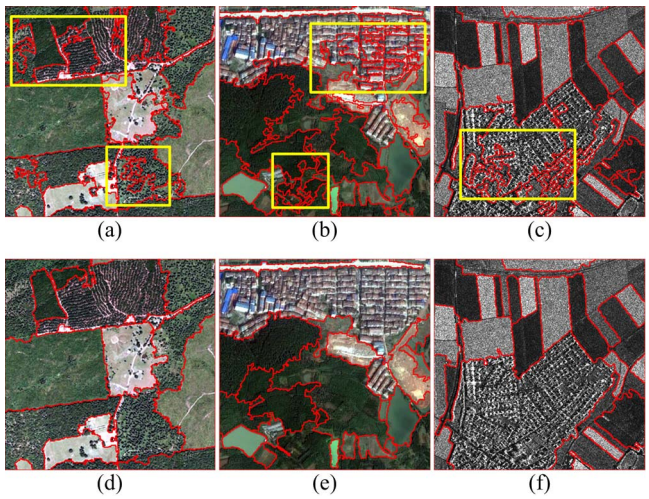

Fig. 2. Segmentation results (400 × 400 pixels, the spatial resolution of the three test images are 2.4, 2.4, and 3 m, respectively). The first row presents the segmentation result without spatial constraint ($\lambda = 0$), and the second row presents the segmentation results with spatial constraint ($\lambda = 0.5$). The merging stop thresholds for the three test images are 19, 24, and 21, respectively.

We set the constraint of shared boundary for regions m and n as follows:

$$D_{m,n} = \frac{1}{\|L_{m,n}\|^{\lambda}} (w_C G_C + w_T G_T) \quad (9)$$

where $\|L_{m,n}\|$ denotes the length of shared boundary of regions m and n and λ is defined as spatial parameter to adjust the constraint of the shared boundary. It can be seen from formulation that, when $\lambda \neq 0$, the pair of adjacent regions with longer shared boundary would be merged with higher priority. This will lead to shorter boundary length and higher compactness of the parent region.

IV. Experiments and Discussions

In this section, experiments and comparisons were carried out to validate the effectiveness of the proposed method, which is implemented using C++ programming language. Several test images are used, including Quickbird, TerraSAR-X, and SPOT-5 images. In order to obtain the fine details of the images, the parameters for EEMW are set as $\alpha = 0.15$, $T = 0.7$, and $area\_threshold = 5$ to get dense oversegmented initial partition, and regions smaller than 50 pixels are merged into their nearest neighborhood based on their color means. The hierarchical merging process is stopped when the number of rest regions is less than a given threshold.

A. Demonstration of Effectiveness of Spatial Constraint

In this experiment, two 2.4-m Quickbird images and a 3-m TerraSAR-X image were used to demonstrate the effectiveness of spatial constraint. The sizes of the test images are 400 × 400 pixels. The merging stop thresholds for each test image are the same with/without spatial constraint. The experimental results are shown in Fig. 2.

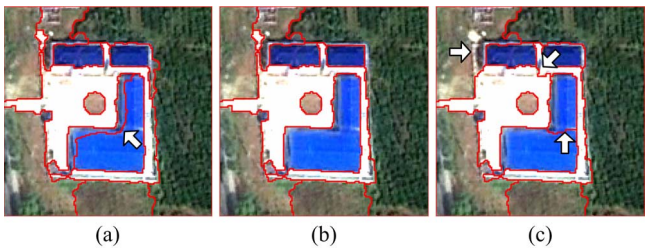

Fig. 3. Segmentation results using different spatial parameters (350 × 350 pixels, 0.6 m/pixel). (a) $\lambda = 0.25$, 11 regions. (b) $\lambda = 0.5$, 11 regions. (c) $\lambda = 0.75$, 11 regions.

Segmentation results without any spatial constraint are shown in the first row of Fig. 2. Many textural areas were oversegmented, as shown in these figures. In addition, many regions had zigzag boundaries, which do not coincide with the actual boundaries of ground objects. This is partially resulted by the high spectral homogeneity values of the initial regions, which will lead to relatively modest importance of textural features. More importantly, when there is no spatial constraint incorporated, the initial regions are merged mainly depending on the spectral distance. Thus, different components of textural areas will be grouped into several subregions with high spectral homogeneity and zigzag boundaries.

The segmentation results with spatial constraint $(\lambda = 0.5)$ are shown in the second row of Fig. 2. From the comparisons, we can see that the spatial constraint can obviously improve the segmentation quality on these textural areas. It is because, under equal conditions, merging priority is given to the couple of regions that share the longest boundary. Thus, different components of textural areas shown in the first row of Fig. 2 will have high merging priorities and be merged together to yield a compact segment hierarchy.

B. Segmentation Using Different Spatial Parameters

It would not be difficult to understand that regions sharing longer boundary will have shorter distance from (9). To reveal the influence of different spatial parameters, a multispectral Quickbird image with a spatial resolution of 0.6 m (fusion product) was used. Following the initial partition, three merging processes using spatial parameters 0.25, 0.5 and 0.75 were applied, respectively. The results are shown in Fig. 3.

As shown in Fig. 3(a), the blue house was segmented into two subregions, among which a narrow ribbon region existed. That is because shared boundary effected slightly, and regions merged mainly based on their color and textural features. An acceptable result using a spatial parameter of 0.5 is shown in Fig. 3(b). As is presented in this figure, almost every object was well partitioned. The merging result using a spatial parameter of 0.75 is shown in Fig. 3(c). The blue house was partitioned into two compact subregions, and the components of the bright bare ground failed to merge together due to their short shared boundary. On the other hand, we can see that the large spatial parameter is not suitable for ribbonlike objects, as is marked on the upper left corner in Fig. 3(c). We suggest that a spatial parameter around 0.5 is fitting for most cases; however, it may change depending on the image content. In addition, we can see that, since the different spatial parameters may effect the merging order of region pairs in different levels, the segmentation outputs may differ a lot, even the numbers of regions are the same.

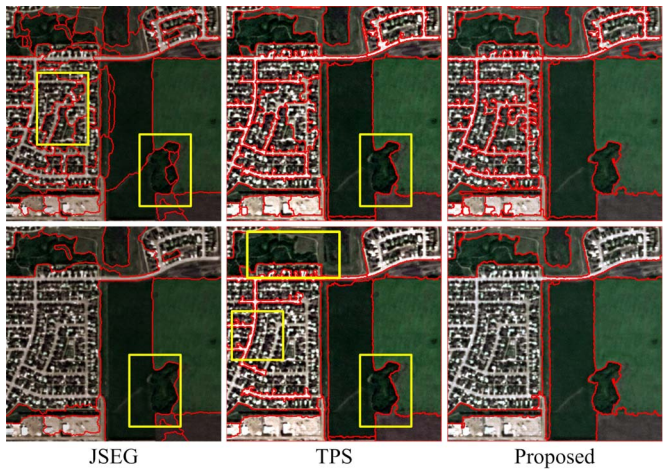

Fig. 4. Experimental results using different methods (350 × 352 pixels, 2.5 m/pixel): JSEG, TPS, and the proposed method. Segmentation results at the finer and coarser levels are presented in the first and second rows, respectively. The parameters of JSEG are $q = 255$ and $m = 0.01$ for the finer level and $q = 255$ and $m = 0.4$ for the coarser level. The merging stop thresholds for TPS and the proposed method are the same, 50 for the finer level and 20 for the coarser level. Some unacceptable segmentation results are marked in the figure.

C. Comparisons on Segmentation Performance

In this section, the proposed method is compared with two color–texture segmentation methods, JSEG method [9] and texture-preceded segmentation (TPS) method [3]. The JSEG source code is available on the Internet (http://vision.ece.ucsb.edu/segmentation/jseg/), and the software for TPS is provided by N. Li. A multispectral SPOT-5 image (350 × 352 pixels, 2.5 m/pixel) is used to evaluate these methods. The spatial parameter used for the proposed method is $\lambda = 0.5$. In order to evaluate the performances on different levels, segmentation results at two different levels are obtained by varying the merging stop threshold. As shown in Fig. 4, the segmentation results at finer level reveal the very fine details, while the results at coarser level point at the skeleton.

As shown in the first column of Fig. 4, the JSEG method failed to get the accurate details at the fine level. The boundaries are not coincided with the real boundaries of the objects. In addition, some areas with similar colors but different textures were undersegmented at both the finer and coarser levels. The results obtained by TPS method are presented in the second column of Fig. 4. The TPS method performed well in getting the fine details of the urban areas. However, it failed to distinguish some areas with similar colors but different textures. When it came to a coarser level, the method was not able to adapt to the different image contents; some areas were undersegmented, while some others are still seriously oversegmented.

As shown in the last column of Fig. 4, the proposed method performed well at both the finer and coarser levels. Areas of different colors and textures were properly partitioned. That is partially contributed by the adaptive weighting of color and textural features, which leads to the full use of the color and

TABLE I
ELAPSED TIME OF THE METHODS (IN SECONDS)

Method	Quickbird1 (400 × 400)	Quickbird2 (400 × 400)	TerraSAR (400 × 400)	SPOT (350 × 350)
JSEG	10.79	10.79	10.152	5.685
TPS	93.5	90.2	88.8	67.26
Proposed	0.977	1.021	0.969	0.703

textural features. On the other hand, as is discussed before, the spatial constraint may contribute a lot to the good performance.

D. Comparisons on Time Efficiency

To evaluate the efficiency of the method, the test images shown in Figs. 2 and 4 are used in this experiment. The computer used in this experiment has an Intel i5 2.4-GHz processor, 2-GB RAM, and Windows XP SP3 operating system. Each experiment is repeated for five times; the average running time of each method applied on different images is presented in Table I. As shown in the table, the proposed method has performed much better than JSEG and TPS methods. Since the calculation of Gabor texture is a time-consuming task, the TPS method suffers the worst time efficiency. Contributed by the high efficiencies of EEMW-, LBP-, and RAG-based region merging processes, the proposed method performs much faster than JSEG and TPS methods. This enables the method suitable for efficient object-based analysis of remote sensing images.

V. CONCLUSION

In this letter, a novel spatially-constrained color–texture segmentation method for VHR remote sensing images has been presented. This method adopts the hierarchical region merging approach and exploits color and textural features and spatial constraint to measure the distances of adjacent regions. Experiments have shown that the method is efficient in overcoming the limitations of the inefficient combination of spatial constraint in color–texture segmentation of VHR images. In addition, comparisons with other methods indicate that the proposed method performs better and much faster than some existing color–texture segmentation methods.

However, image segmentation is still an ill-posed problem, as the level at which the segmentation is to be performed depends on each application. Although in computer vision applications there are already reference data sets for image segmentation such as the Berkeley data set, the same does not happen with remote sensing applications. Moreover, it is difficult to generally evaluate the performance of a certain segmentation method in a quantitative manner. Thus, a qualitative analysis by a visual comparison is carried out to evaluate the proposed method. Acknowledged evaluate criterions as well as reference data sets are needed for evaluating segmentation methods for remote sensing applications.

The selection of thresholds for multiresolution image segmentation is still an intractable problem. In this method, the merging process is stopped when the number of the rest regions is smaller than a given threshold. It loses a meaningful explanation and may not be suitable for large-size images. Thus, research on quantitative methods for selecting thresholds is potential in our future work.

ACKNOWLEDGMENT

The authors would like to thank Dr. X. Wu (Commonwealth Scientific and Industrial Research Organisation Mathematical and Information Sciences for his valuable comments and advices, N. Li (Shanghai Jiao Tong University) for providing evaluating software, and the anonymous reviewers for their highly constructive and outstanding remarks.

REFERENCES

[1] T. Blaschke, "Object based image analysis for remote sensing," *ISPRS J. Photogramm. Remote Sens.*, vol. 65, no. 1, pp. 2–16, Jan. 2010.
[2] T.-S. Roger, S. Georges, L. Jean, and A. K. Katsaggelos, "Using colour, texture, and hierarchical segmentation for high-resolution remote sensing," *ISPRS J. Photogramm. Remote Sens.*, vol. 63, no. 2, pp. 156–168, Mar. 2008.
[3] N. Li, H. Hong, and T. Fang, "A novel texture-preceded segmentation algorithm for high-resolution imagery," *IEEE Trans. Geosci. Remote Sens.*, vol. 48, no. 7, pp. 2818–2828, Jul. 2010.
[4] U. C. Benz, P. Hofmann, G. Willhauck, I. Lingenfelder, and M. Heynen, "Multi-resolution, object-oriented fuzzy analysis of remote sensing data for GIS-ready information," *ISPRS J. Photogramm. Remote Sens.*, vol. 58, no. 3/4, pp. 239–258, Jan. 2004.
[5] R. Gaetano, G. Scarpa, and G. Poggi, "Hierarchical texture-based segmentation of multiresolution remote-sensing images," *IEEE Trans. Geosci. Remote Sens.*, vol. 47, no. 7, pp. 2129–2141, Jul. 2009.
[6] A. Mecocci, P. Gamba, and A. Marazzi, "Texture segmentation in remote sensing images by means of packet wavelets and fuzzy clustering," in *Proc. SPIE*, Sep. 1995, vol. 2584, pp. 142–151.
[7] X. Hu, C. V. Tao, and B. Prenzel, "Automatic segmentation of high-resolution satellite imagery by integrating texture–intensity and color features," *Photogramm. Eng. Remote Sens.*, vol. 71, no. 12, pp. 1399–1406, Dec. 2005.
[8] A. Wang, S. Wang, and A. Lucieer, "Segmentation of multispectral high-resolution satellite imagery based on integrated feature distribution," *Int. J. Remote Sens.*, vol. 31, no. 6, pp. 1471–1483, Feb. 2010.
[9] Y. Deng and B. S. Manjunath, "Unsupervised segmentation of color–texture regions in image and video," *IEEE Trans. Pattern Anal. Mach. Intell.*, vol. 23, no. 8, pp. 800–810, Aug. 2001.
[10] C. Carson, S. Belongie, H. Greenspan, and J. Malik, "Blobworld: Image segmentation using expectation-maximization and its application to image querying," *IEEE Trans. Pattern Anal. Mach. Intell.*, vol. 24, no. 8, pp. 1026–1038, Aug. 2002.
[11] Z. Kato and T. C. Pong, "A Markov random field image segmentation model for colour texture images," *Image Vis. Comput.*, vol. 24, no. 10, pp. 1103–1114, Oct. 2006.
[12] Z. Wang and R. Boesch, "Color- and texture-based image segmentation for improved forest delineation," *IEEE Trans. Geosci. Remote Sens.*, vol. 45, no. 10, pp. 3055–3062, Oct. 2007.
[13] T. Ojala, M. Pietikainen, and D. Harwood, "A comparative study of texture measures with classification based on feature distributions," *Pattern Recognit.*, vol. 29, no. 1, pp. 51–59, Jan. 1996.
[14] T. Ojala, M. Pietikainen, and T. Maenpaa, "Multiresolution gray-scale and rotation invariant texture classification with local binary patterns," *IEEE Trans. Pattern Anal. Mach. Intell.*, vol. 24, no. 7, pp. 971–987, Jul. 2002.
[15] K. M. Chen and S. Y. Chen, "Color texture segmentation using feature distributions," *Pattern Recognit. Lett.*, vol. 23, no. 7, pp. 755–771, May 2002.
[16] K. Haris, S. N. Efstratiadis, M. Maglaveras, and A. K. Katsaggelos, "Hybrid image segmentation using watersheds and fast region merging," *IEEE Trans. Image Process.*, vol. 7, no. 12, pp. 1684–1699, Dec. 1998.
[17] J.-M. Beaulieu and M. Goldberg, "Hierarchy in picture segmentation: A stepwise optimization approach," *IEEE Trans. Pattern Anal. Mach. Intell.*, vol. 11, no. 2, pp. 150–163, Feb. 1989.
[18] J. Benediktsson, L. Bruzzone, J. Chanussot, M. Mura, P. Salembier, and S. Valero, "Hierarchical analysis of remote sensing data: Morphological attribute profiles and binary partition trees," *Proc. 10th Int. Conf. Math. Morphol. Appl. Image signal Process.*, vol. 6671, pp. 306–319, 2011.
[19] D. Li, G. Zhang, Z. Wu, and L. Yi, "An edge embedded marker-based watershed algorithm for high spatial resolution remote sensing image segmentation," *IEEE Trans. Image Process.*, vol. 19, no. 10, pp. 2781–2787, Oct. 2010.
[20] D. E. Ilea and P. F. Whelan, "Color image segmentation using a self-initializing EM algorithm," in *Proc. 6th Int. Conf. Vis., Imag. Image Process.*, Aug. 2006, pp. 417–424.